Arch. Metall. Mater. **70** (2025), 1, 341-350

DOI: https://doi.org/10.24425/amm.2025.152551

Y. TAJUNNISA[1*], A.K. APSARI[2], R. BAYUAJI[1], MOH. SAFI'I MANSUR[2]

THE IMPACT OF LONGITUDINAL AND STIRRUPS REINFORCEMENT RATIO TO SHEAR STRENGTH CAPACITY OF GEOPOLYMER CONCRETE BEAM

The shear capacity of reinforced beam concrete was designed to resist the stirrup reinforcement, *Vs*, and by the concrete itself, *Vc*. Previous studies of geopolymer concrete show the mechanical properties of this proposed green concrete, yet the structural investigation is infrequently investigated. These studies mostly observed the impact of using alternative binder resources that affect the workability, setting time, compressive strength, split tensile strength, and drying shrinkage. Therefore, this study aims to observe the structural behavior of geopolymer concrete, precisely its shear capacity. Four geopolymer concrete beam types were designed to have shear failure mode when tested using a Universal Testing Machine by four-point load bending method. The results showed that geopolymer concrete has ductile behavior. Comparison between the *Vu* value of the test results with *Vn* calculation of nominal cross-sectional capacity according to standard concrete rules in an average of 2.11 higher than the nominal capacity conventionally calculated according to SNI. Two models of linear regression equations for concrete *Vc* values were created to explore this further. It was found that the presence of a constant increases the value of the coefficient of determination by up to 29% for the *Vc* equation in geopolymer concrete. In addition, cracking patterns observed with the DIC method using GOM Correlate software also showed that all the beam specimens had failure both in flexure and shear, even though they all are designed in a shear failure state.

Keywords: Geopolymer Concrete; Beam; Reinforcement; Shear Strength; Fly Ash

1. Introduction

Research on innovative and sustainable materials in structural engineering and construction has led to the development of geopolymer concrete, a new and eco-friendly alternative to traditional Portland cement-based concrete [1]. Geopolymer concrete, derived from industrial by-products such as fly ash and slag, offers exceptional potential for reducing carbon emissions and enhancing infrastructure longevity [2]. A critical aspect of assessing the viability of any concrete material, including geopolymer concrete, is its shear strength capacity, particularly in beams, which are fundamental structural components in many buildings and infrastructure [3].

Shear strength is the capacity of a material to resist lateral forces that cause it to slide or deform, one of the crucial parameters for structural stability [4]. Regarding geopolymer concrete beams, two essential factors are pivotal in determining their shear strength: adequate depth and reinforcement formation. The ratio of these reinforcement components, their arrangement, and their properties significantly impact the overall performance of the geopolymer concrete beams [5,6].

This study explores and analyzes the influence of longitudinal and stirrups reinforcement ratios on the shear strength capacity of geopolymer concrete beams. By understanding how these factors affect such beams' structural integrity and load-carrying capabilities, engineers and researchers better optimize their design and construction processes, ultimately leading to more sustainable and resilient infrastructure.

Investigating shear strength in geopolymer concrete beams is paramount, especially when environmental concerns and sustainability are at the forefront of construction practices. Geopolymer concrete offers great promise in reducing carbon emissions and waste in the construction industry [7]. Therefore, a thorough understanding of the factors that affect the shear strength capacity of geopolymer concrete beams is vital to ensure their widespread acceptance and utilization in practical applications.

This research interprets the intricate relationship between reinforcement ratios, geopolymer concrete's unique properties,

[1] CIVIL INFRASTRUCTURE ENGINEERING DEPARTMENT, FACULTY OF VOCATIONAL STUDIES, INSTITUTE TECHNOLOGY OF SEPULUH NOPEMBER, SURABAYA, 60111, INDONESIA
[2] CIVIL ENGINEERING DEPARTMENT, FACULTY OF CIVIL, PLANNING, AND GEO-ENGINEERING, INSTITUTE TECHNOLOGY OF SEPULUH NOPEMBER, SURABAYA, 60111, INDONESIA

* Corresponding author: yuyun_t@ce.its.ac.id

and shear strength, providing a solid foundation for further advancements in developing and implementing this eco-friendly building material. The findings of this study have the potential to transform the way we approach concrete construction, enhancing its sustainability and resilience while contributing to a greener and more environmentally responsible future.

2. Materials and methods

Several procedures were conducted to observe the shear capacity. Four beam samples were designed with a shear failure. Thus, the *P* ultimate flexure is greater than the *P* maximum shear. Based on this calculation, the reinforcement variables were decided. This also leads to the mixed design proportion with the targeted value of *fc'* matching the initial estimate. Then, the casting and curing process is followed to aim for the optimum value of *fc'* at 28 days old. Aside from the beam samples, cylindrical samples were also produced to gain the compression value of *fc'* of concrete.

The beam testing code is ACI 318 for flexural tests with a four-point load bending method. This method is chosen by the shear span that occurs due to the position of point loading between each end joint of the beam with the load points, as illustrated by Fig. 1. The crack pattern that occurred during the loading test was also observed by Digital Image Correlation method using an opensource software namely GOM by ZEUSS.

2.1. Shear Design Capacity

According to Indonesian National Standards (SNI), several equations were used to calculate the shear design capacity so that all the beams observed had a shear failure condition. These equations are shown in Eqs. (1)-(6).

$$Pu_{flexure} > Pu_{shear} \tag{1}$$

$$Pu_{flexure} = \frac{2\left(Mu - \frac{1}{8}qu \cdot L^2\right)}{a} \tag{2}$$

$$Pu_{shear} = 2 \cdot Vu \tag{3}$$

$$Vu = Vc + Vs \tag{4}$$

$$Vc = 0{,}17 \cdot \sqrt{fc} \cdot bw \cdot d \tag{5}$$

$$Vs = \frac{Av \cdot fy \cdot d}{s} \tag{6}$$

Where:

- *Pu* – Ultimate element force (N),
- *fy* – Steel tensile strength (MPa),
- *Mu* – Ultimate bending moment (N),
- *d* – Effective depth (mm),
- *Vu* – Ultimate shear strength of the element (N),
- *bw* – width of the cross section (mm),
- *Vc* – Shear strength provided by concrete (N),
- *Av* – Shear reinforcement area per millimeter span (mm^2),
- *Vs* – Shear strength provided by stirrups (N),
- *fc* – Concrete compressive strength (MPa),
- *s* – Space between each stirrup reinforcement (mm).

A shear failure mode is required to investigate the shear behavior of beam specimens. Thus, the flexure-designed capacity of the cross-section area must be higher than the shear capacity, as shown in Eq. (1). In the experimental testing procedure, the UTM (Universal Testing Machine) pushed the ultimate force (*Pu*) at the center of the system, this force continuously loads

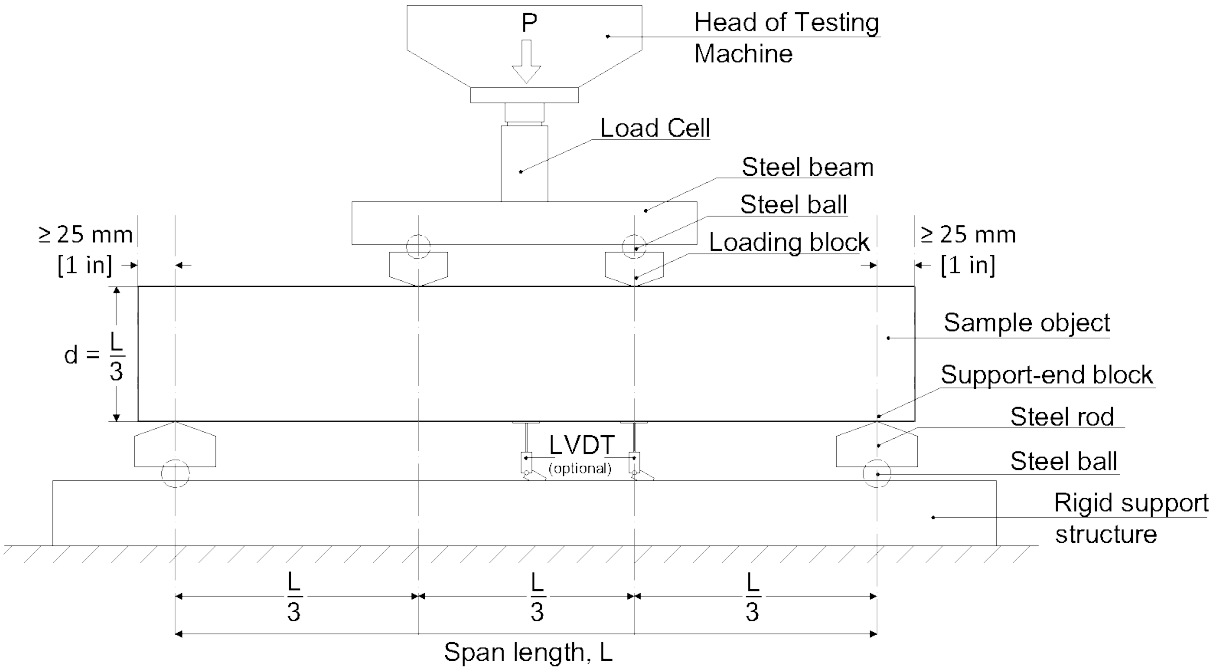

Fig. 1. Four-point load bending set up according to ACI 318

the two-point loading block of the beam with a span of L/3 mm (Fig. 1). Therefore, the actual ultimate shear force from the UTM is half the ultimate force (Eq. (3)). The shear force directed to the beam is supported by the shear reinforcement/stirrups and the concrete itself. The calculation of the concrete shear capacity is based on empirical formulas obtained from previous research experiments, resulting in Eq. (5) with a constant value of 0.17. Conversely, the shear capacity supported by the stirrups is determined by calculating the area of stirrup reinforcement per unit distance, as indicated in Eq. (6).

The preliminary design parameters to calculate in those equations used include section and rebar properties. The beam specimens' section properties are rectangular cross-sections of 150 mm of width, 250 mm of height, and 1800 mm of length. The concrete cover thicknesses are set up at 20 mm, and the compressive strength value of fc' is 35 MPa. Whereas for the rebar properties parameters, the steel tensile strength of longitudinal reinforcement is 420 MPa, while the stirrups reinforcement is 240 MPa with a diameter of 16 mm and 6 mm, respectively.

Using those parameters, the different variables of the rebar were compared, especially the longitudinal and stirrups ratios. Four beams with varying rebar reinforcements were examined, as shown in TABLE 1. Specimens 1A and 2B are then compared to see the effect of longitudinal reinforcement toward shear behavior capacity. Specimen 1A and 1B have different stirrup formations, while 1C has no stirrups. These beams are compared to observe the stirrup bar reinforcement toward shear behavior and capacity. Fig. 2 shows the beam specimens to illustrate the designated parameters.

TABLE 1

Shear failure design capacity

Beam Specimen Types		1A	1B	2B	1C	Unit
longitudinal (D)	top	2	2	2	2	pcs
	bot	2	2	3	2	
As	top	56.55	56.55	56.55	56.55	mm²
	bot	402.12	402.12	603.19	402.12	
a		37.85	37.85	37.85	56.77	mm
Mn = Mu		33.28	33.28	33.28	47.53	kN.m
Pu flexure		131.71	131.71	131.71	188.69	kN
Stirrups (ø)	n	10	8	8	—	pcs
	s	200	250	250	—	mm
Av		47.12	47.12	37.70	—	mm²
Vs		12.21	12.21	7.82	—	N
Vc designed		32.59	32.59	32.59	32.59	kN
Vu		44.80	44.80	40.40	40.40	kN
Pu shear		89.60	89.60	80.81	80.81	kN
ρ longitudinal		0.0107	0.0107	0.0107	0.0161	—
ρ shear (stirrups)		0.0013	0.0013	0.0010	0.0010	—

2.2. Mix Design Proportions

Based on T. Phoo-ngernkham's research, the mix design procedure is presented in Eqs. (7)-(14). This procedure demands

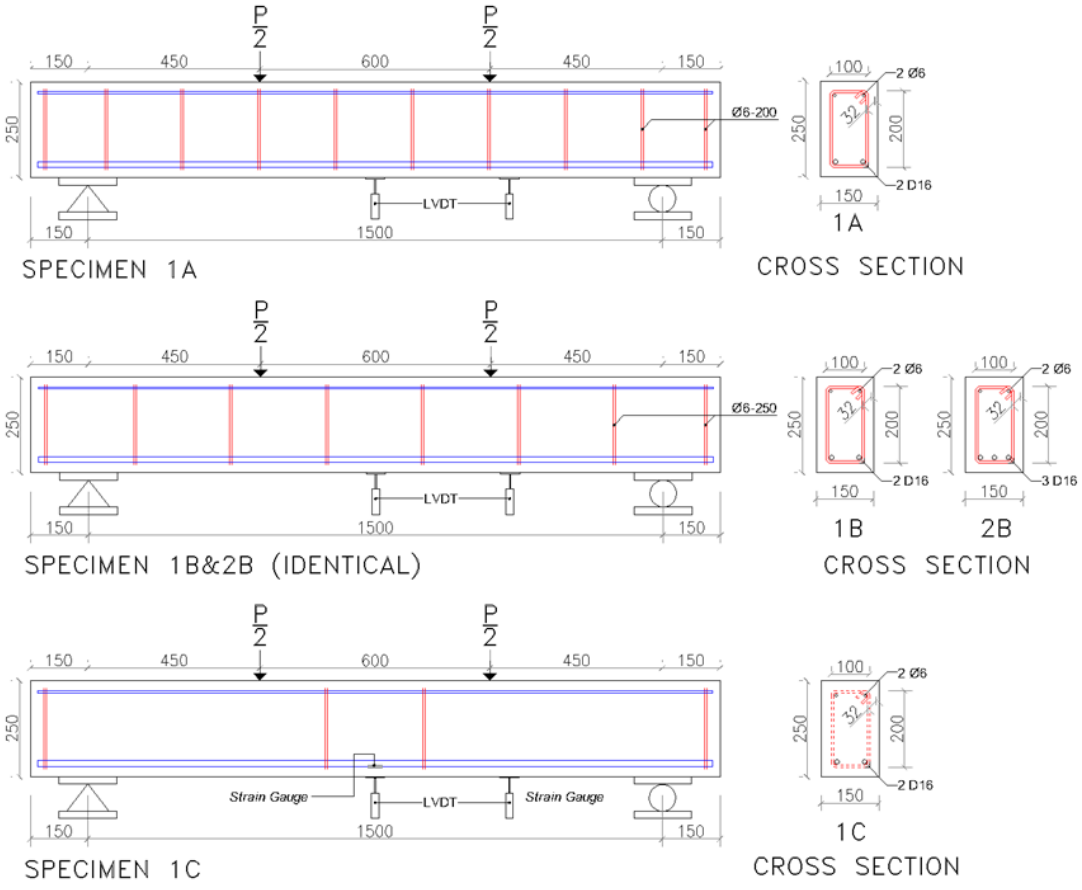

Fig. 2. Designed specimens drawing

several material test results, such as specific gravity and maximum size gradations of coarse and fine aggregates. Therefore, certain material tests were conducted with the results shown in TABLE 3. The alkali activator used is 12 M; thus, with the basic concepts of molarity, as shown in Eq. (7), NaOH flakes (solid) for every 1 liter of water is 480 grams. To calculate the amount of water needed, the maximum water content is determined based on the maximum aggregate size and the percentage of voids, as presented in ngernkham's research (TABLE 2). Therefore, the maximum water content per cubic meter of concrete is 200 kg/m^3. AAS_{adj} is alcaline activator solution adjustment due to the water content absorbed by the fine aggregates, as described in Eq. (8). Lastly, to retrieve the total amount of alcaline activator solution (*AAS*), simply sum up the amount of water needed and AAS_{adj} (Eq. (9)). Similar to the ordinary concrete mix design, where the water-to-cement (W/C) ratio is a key factor in achieving the targeted compressive strength, in geopolymer concrete, the alkaline activator solutions-to-fly ash (*AAS*/FA) ratio plays the same role. Fig. 3 shows the influence of *AAS*/FA ratio according to 28-day compressive strength according to *T*. Phoo-ngernkham's work. To achieve targeted compressive strength of 35 MPa, the AAS/FA ratio should be 0.45, and the fly ash content can be obtained through Eq. (10). It should be noted that the alkaline activator solution consists of two compounds, sodium hydroxide and sodium metasilicate, in a 1:1 ratio. Using Eq. (11), we can determine the amount of each compound per cubic meter. The amounts for both coarse and fine aggregates can be determined from Eqs. (12) and (13), respectively. Finally, the admixture retardamt dosage is calculated using Eq. (14) [8].

TABLE 2

Maximum water content and percentage of air per cubic meter of concrete [8]

Max. size of aggregates	Max. water cont. (kg/m^3)	Precentage / Void (%)
10	225	3,0
12,5	215	2,5
20	200	2,0

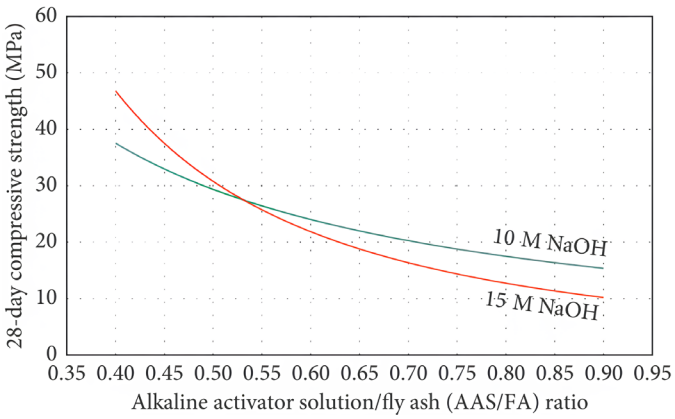

Fig. 3. Twenty-eight-day compressive strength versus the AAS/FA ratio curve [8]

TABLE 3

Material test result

Parameter	Coarse Aggregates	Fine Aggregates	Fly Ash	NaOH	Na_2SiO_3
Max. size aggregates (mm)	20	4.76	—	—	—
Specific gravity (kg/m^3)	2712.7	2743.1	2750.3	1132	1554.7
Moisture content (%)	1.59	6.38	—	—	—
Absorption (%)	1.54	0.17	—	—	—

$$M = \frac{gr}{Mr} \times \frac{1}{V} \tag{7}$$

$$AAS_{Adj} = \left| \left\{ \left[1 - \left(\frac{\rho_{RS}}{S_G \cdot \rho_w} \right) \right] \times 100 \right\} - 35 \right| \times 4,75 \tag{8}$$

$$AAS = Max.water + AAS_{Adj} \tag{9}$$

$$Fly\ ash = \frac{AAS}{AAS\ /\ FA\ ratio} \tag{10}$$

$$\mathrm{Na_2SiO_3} = \frac{AAS}{\left[1 + \left(\frac{1}{(\mathrm{Na_2SiO_3} / \mathrm{NaOH})} \right) \right]} \tag{11}$$

$$M_{RS} = 0,3 S_{G(RS)} \left[\begin{matrix} 1 - V_{FA} - V_{\mathrm{NaOH}} - \\ V_{\mathrm{Na_2SiO_3}} - V_{water} \end{matrix} \right] \times 1000 \tag{12}$$

$$M_{LS} = 0,7 S_{G(LS)} \left[\begin{matrix} 1 - V_{FA} - V_{\mathrm{NaOH}} - \\ V_{\mathrm{Na_2SiO_3}} - V_{water} \end{matrix} \right] \times 1000 \tag{13}$$

$$SP = \left(\frac{1}{100} \times Fly\ Ash \right) \tag{14}$$

Where:

M – molar concentration,
M_{RS} – coarse aggregates (kg/m^3),
gr – solids of compound,
$S_{G(RS)}$ – Specific gravity of coarse aggregates (kg/m^3),
Mr – relative atomic masses,
M_{LS} – fine aggregates (kg/m^3),
v – per litre of volume,
$S_{G(LS)}$ – Specific gravity of fine aggregates (kg/m^3),
ρ_{RS} – density of the fine aggregate in SSD condition (kg/m^3),
V_{FA} – volume of fly ash (kg/m^3),
V_{NaOH} – volume of sodium hydroxide (kg/m^3),
S_s – specific gravity (kg/m^3),

$V_{Na_2SiO_3}$ – volume of sodium metasilicate (kg/m^3),
ρ_w – density of water (kg/m^3),
V_{water} – volume of water (kg/m^3).

TABLE 4

Mix design proportions

Fly Ash	=	669.28	kg
Fine aggregates	=	449.98	kg
Coarse aggregates	=	1051.51	kg
NaOH	=	133.86	kg
Na_2SiO_3	=	133.86	kg
Retardant Admixture (Sucrose)	=	6.69	kg
Concrete density	=	2445.18	kg/m^3

2.3. Casting and Curing

The manufacture of concrete test objects is carried out in the ITS Building Materials and Structures Laboratory. The following step in the process is the casting phase. Next, all the materials are measured following the mold or formwork volume, following the mix design proportions. Combine the fly ash and alkali activators (NaOH $_{[S]}$ $Na_sSiO_{3\ [S]}$) in a milling machine resulting in a dry mixture namely geopolymer cement [9]. Pour this cement and both aggregates into the concrete mixer and ensure they are thoroughly mixed, which usually takes about 5 minutes. It's crucial to confirm that the aggregates are in a surface-saturated dry (SSD) condition in which the aggregate pores have been filled with water, but the surface remains dry. This condition prevents early reactions caused by the highly reactive fly ash and alkali activators, which can lead to rapid setting. Additionally, saturated pores help prevent the concrete from shrinking internally during and after the reaction. To achieve an SSD condition of the aggregates according to ASTM C 127-01, firstly wash them thoroughly to remove dust and dirt from the surfaces. Then, submerge the aggregates for 24 hours to fill the pores and satisfy the absorption. Then, rinse and dry the surface using a towel, or simply wait until the surface is not wet but the color of the aggregates remains dark. This indicates that each aggregate is content with water; thus, the polymerization process can form optimals during the reaction process. After the aggregates are ready, add the water and wait approximately four more minutes while closely monitoring the mixture's consistency and workability. Lastly, pour the admixture into the mix; in this case, the author uses sucrose as a retardant admixture that is proven to enhance the workability of fresh geopolymer concrete. The amount of admixture used is one percent of the fly ash mass [8,10]. Continue mixing for a couple of minutes before pouring the fresh geopolymer concrete into the formwork [9].

The slump test assessed workability, which correlates with fluidity of the fresh concrete. In this study, the target for the slump test was set at 200±20 mm. Subsequently, the fresh concrete was poured into the formwork and cylinder mold, both coated with oil. Various tools like a rubber hammer and concrete vibrator compacted the fresh concrete. Geopolymer concrete boasts distinct characteristics, one of which pertains to its curing process. In contrast to Portland cement concrete, which is ideally cured with water, geopolymer concrete can be cured effectively at ambient to dry temperatures [11,12]. Therefore, in this research, the curing process occurs at room temperature, typically 30-35°C, and is shielded with a tarp to safeguard it from external disturbances.

2.4. Test Set-up

In the testing process, the beam specimen was carefully placed onto the UTM that supported it with the assistance of a mini crane. A camera mounted on a tripod was set to automatically capture images at five-second intervals. To observe the displacement, 2 LVDTs (Linear Variable Differential Transformer) were positioned in the middle of the beam's span and below the load point, with cables connected to the data logger channels. With the UTM machine activated, loading numbers were displayed on the monitor as the load increased, causing cracks to lengthen and widen progressively. The ultimate condition of the beam was marked by a sudden, pronounced crack and a loud noise, prompting the cessation of the UTM machine's loading. Subsequently, the beam was lowered from the UTM machine, and photographs were taken to document the cracks formed during the testing process [12].

Fig. 4. Casting process and slump test of beam specimens

Fig. 5. Beam test set up for four-point load bending

3. Results

3.1. Compressive and Tensile Test

Compressive strength tests were carried out to determine the fc' value. TABLE 5 shows the average concrete compressive strength values for all the beam specimens at 28 days old.

TABLE

Compressive test result from cylindrical specimen of each beam

Specimen	fc_1	fc_2	fc_3	fc'
1A	58.19	45.84	50.67	51.57
1B	57.81	59.08	57.81	58.23
2B	60.99	57.04	55.00	57.68
1C	54.24	61.88	58.44	58.19

3.2. Load-deflection curve

Some data is obtained from the testing process, including load and deflection, that can be calculated to determine the shear capacity of each beam. The ultimate load is obtained by finding the maximum value of the load cell reading for each beam test, which occurs when the beam fails. Usually, this failure occurs after the beam has experienced a long yield condition and is suddenly characterized by a large deflection and a loud sound. TABLE 6 shows a recapitulation of the ultimate load results and compares them with the nominal shear capacity of each beam.

The designed Pu and *Vn* are obtained from the calculations in TABLE 1 with the *fc'* and *fy* values similar to the designed parameters. The Pu and *Vu* tests are obtained from the data logger connected to the load cell, which results from testing until the failure cracks. The actual *Vn* is obtained from the same calculation method as in TABLE 1. Still, the concrete compressive strength (*fc'*) and steel tensile strength (*fy*) are according to each beam's cylinder compressive strength test results and the steel tensile tests shown in TABLES 4 and 5, respectively. It can be said that the actual *Vn* is the capacity of the cross-section in the existing condition according to the actual quality.

One of the observable results of the four-point load bending test is the load-deflection curve. This curve presents the deflection data in the beam when given a monotonous *P* load. This load reading is calibrated and combined with the deflection reading from the LVDT by the data logger. Fig. 5 displays the load and deflection interaction for all beam specimens.

TABLE 6

Steel tensile strength

Sample	D (mm)	A (mm²)	L0	L1	e	Py	Pu	Fy	Fu
			(mm)		(%)	(kN)		(MPa)	
1 ø6	5.59	24.542	200	235.10	17.5	12.00	14.60	489	595
2 ø6	5.61	24.718	200	234.65	17.5	11.40	14.20	461	574
3 ø6	5.64	24.983	200	229.40	14.5	12.00	14.70	480	588
1 D16	15.71	193.839	200	231.30	15.5	93.20	119.00	481	614
2 D16	15.69	193.346	200	231.75	16	92.50	119.30	478	617
3 D16	15.67	192.854	200	234.50	17	91.20	118.60	473	615

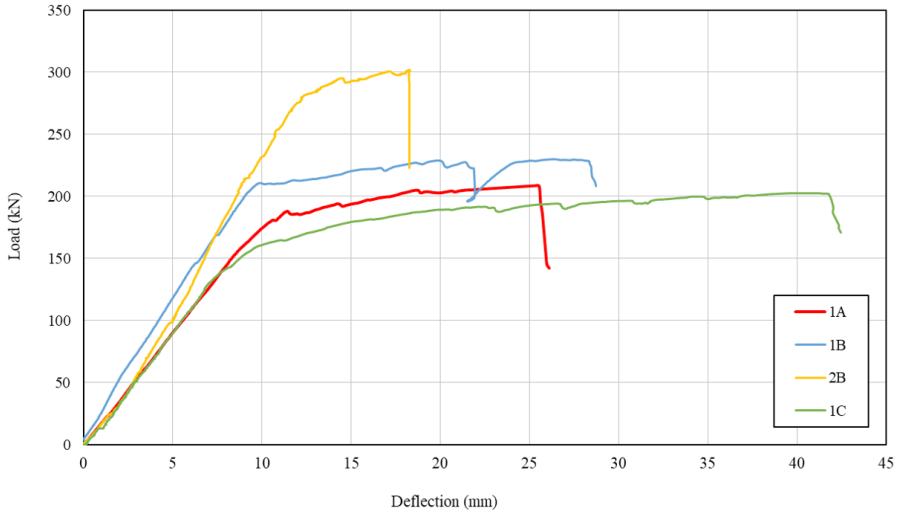

Fig. 6. Load deflection curve

TABLE 7

Ultimate loading test result

Test Result (kN)	Specimen			
	1A	1B	2B	1C
Pu designed	131.71	131.71	188.69	131.71
Vn designed	44.80	40.40	40.40	32.59
Pu test	208.67	230.07	302.02	202.36
Vu test	104.34	115.04	151.01	101.18
Vn real	63.81	57.56	57.36	42.02
Vu test / *Vn* real	1.64	2.00	2.63	2.41
Max deflection (mm)	26.10	28.72	18.32	41.16

Beams 1A, 1B and 1C have the same flexural reinforcement configuration of 2-D16 for tensile reinforcement and 2-ø6 for compressive reinforcement. The difference lies in the shear reinforcement or stirrups. Beam 1A has ø6-200 stirrups, beam 1B has ø6-250, and beam 1C has no stirrups. These three beams were compared to determine the performance of the beams in carrying the load and the deflection that occurred, as shown in Fig. 5.

It can be seen that beam 1B, with more spaced stirrups, could carry a higher *Pu* value than 1A. However, 1A is more ductile as it is able to withstand a larger deflection with constant *Pu*. Beam 1C has the least *Pu* among the other three beams and is the most brittle. This can be observed from the large deflection of beam 1C that occurs with constant P.

The observation of beam 1B and beam 2B have the same variation of stirrup reinforcement, namely ø6-250, but different variations of flexural reinforcement. Beam G1B has 2-D16 tensile reinforcement, while beam 2B has 3-D16. As shown in Fig. 4.9, beam 2B has a Pu value of 24% greater than beam 1B. This occurs because more flexural reinforcement makes the As value increase and impacts the cross-sectional capacity value of the 2B beam. However, 1B beams can bear a more extended deflection than 2B beams. The phase from yield to failure is also shorter for 2B beams than for 1B beams.

3.3. Shear Strength Capacity Analysis

In the LRFD structural element design, a reduction factor (φ) that acts as a designed safety factor. However, in this study, the reduction factor can be ignored. Thus, *Vu* (*V* ultimate) is considered equal to *Vn* (*V* nominal), where *Vu* is obtained from the *P* ultimate test and *Vn* is the result of calculating the cross-section capacity according to SNI. *Vn* is the sum of the shear capacity carried by concrete (*Vc*) with that carried by shear reinforcement or stirrups (*Vs*), as shown in Eq. (4).

The *Vc* obtained from the test results with the *Vc* calculated by SNI (Indonesians' National Standards) has a considerable difference, of 2-3 times. However, to find out why this happened, an analysis approach was conducted to determine the effect of the coefficient 0,17 on the *Vc* of the test samples. It is possible that the coefficient of 0,17 is less relevant for geopolymer concrete, and a different coefficient or even calculation is required.

TABLE 8

Comparison of *Vc* test with *Vc* SNI

Beam Specimen	*Pu* (kN)	*Vu* (kN)	*Vs* (kN)	*Vc* test (kN)	*fc* (MPa)	*Vc* SNI (kN)	*Vc* test/ *Vc* SNI
	A	B	C [Eq. (6)]	D D = B-C	E	F [Eq. (5)]	
1A	208.67	104.34	24.26	80.08	51.57	39.55	2.02
1B	230.07	115.04	15.53	99.51	58.23	42.03	2.37
2B	302.02	151.01	15.53	135.48	57.68	41.83	3.24
1C	202.35	101.18	0.00	101.18	58.19	42.02	2.41

Approach analysis is done by modeling the results of the *Vc* test and *Vc* SNI values into a linear graph. Eq. (16) shows that the *Vc* value is directly proportional to the square root value of the concrete quality multiplied by the effective cross-sectional area. In linear equations, the concept is shown in equation 15 where a is the gradient of the linear line equation, and b is a constant. When applied to Eq. (17), the y-value is *Vc*, and the x-value is $\sqrt{fc} \cdot bw \cdot d$ with $\lambda = 1$. With this concept, the value of a, which is a coefficient of 0.17, can be obtained. For that, it is supposed:

$$y = ax + b \tag{15}$$

$$Vc = z \cdot \left(\sqrt{fc} \cdot bw \cdot d\right) \tag{16}$$

$$y = a \cdot \mathrm{x} \tag{17}$$

After obtaining the x and y values, a linear regression can be made to determine the equation and gradient. TABLE 9 presents the x and y values for each beam sample, while Fig. 7 displays the linear regression equation obtained from the graphical of TABLE 9.

Model 1, uses a straight regression line of Eqs. (18) and (19) with a constant '*b*' according to Eq. (15). The *Vc* of the test approach is different from the conventional calculation *Vc* of SNI. In *Vc* SNI (Eq. (19)), the value of the constant b is insignificant, contradictory to the *Vc* test in Eq. (18), and is much greater, affecting the magnitude of the *Vc* value. Model 2 uses the approach according to the equation in SNI (Eq. (17)) because there is no constant value b, listed in Eqs. (20) and (21). The coefficient x for *Vc* SNI between model 1 and model 2 is 0.17. However, in the *Vc* test, the coefficient x is 2.5 times smaller than model 1. Therefore, the regression line is declining because the gradient is smaller.

TABLE 9

Ordinate and axis value for linear regression analysis

Beam Specimens	Fc'	$\sqrt{fc'}$	x	y	
			$\sqrt{fc} \cdot bw \cdot d$	*Vc* test	*Vc* SNI
	MPa		kN	kN	kN
1A	51.57	7.18	232.66	80.08	39.55
1B	58.23	7.63	247.24	99.51	42.03
2B	57.68	7.59	246.06	135.48	41.83
1C	58.19	7.63	247.15	101.18	42.02

TABLE 10

Linear regression for constitutive model equations

Equation	Model 1		Model 2	
	$y = ax + b$		$y = a \cdot x$	
Vc test	$y = 1.053x - 151.55$	(18)	$y = 0.406x$	(20)
Root square	$R^2 = 0.7418$		$R^2 = 0.4586$	
Vc SNI	$y = 0.17x - 5 \cdot 10^{-13}$	(19)	$y = 0.17x$	(21)
Root square	$R^2 = 1$		$R^2 = 1$	

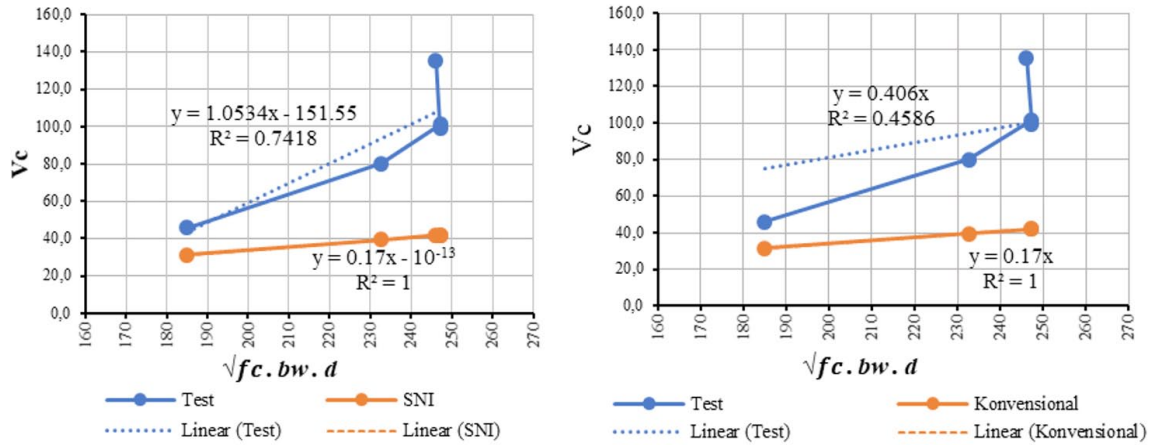

Fig. 7. Linear regression model 1 (left) and model 2 (right)

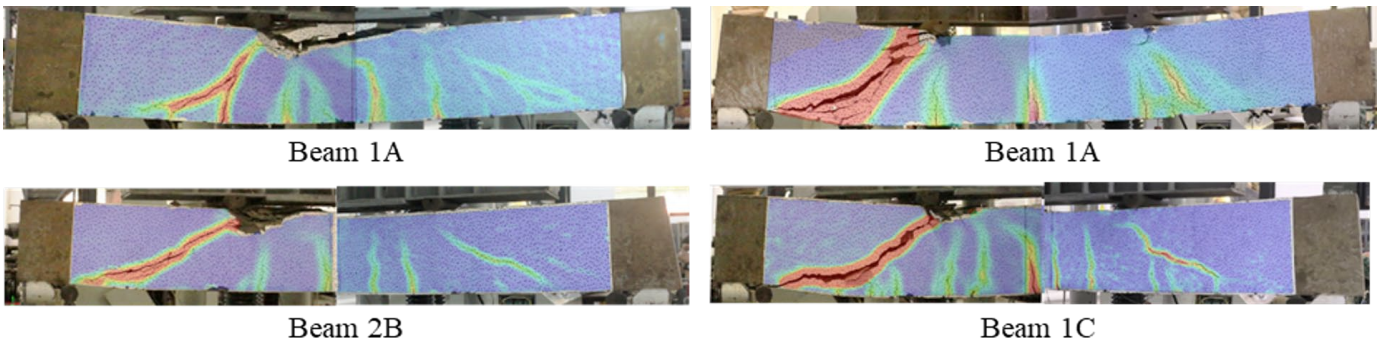

Fig. 8. Beams crack pattern after ultimate failure condition analyzed with Digital Image Correlation method

To compare the model quality among these four equations, consider the coefficient of determination. The coefficient of determination in regression equations assesses the fit between the original data and the model, also known as the root square (r^2). Root square is a value to evaluate how strongly the independent variable affects the response variable in the data. The higher the r^2, the better the model. According to [13], r^2 values are grouped into several categories: ≤0.75 as strong, ≤0.5 as moderate, and ≤0.25 as weak. Vc SNI has a perfect r^2 value of 1 (Eqs. (19) and (21)). This is because calculating *Vc* SNI using a formula with a coefficient of 0.17, causes the response variable (*y*) to be directly influenced by the independent variable (*x*). Thus, the graph will show a perfect coefficient of determination. The achievement of the *Vc* test model 1 results shows a correlation of 74% between the response variable and the independent variable. The constant value in model 1 is 60%, while in model 2, it is only 45%. The most striking difference between models 1 and 2 lies in the constant value. With the continuous, the modeling interpretation increased by 29% compared to without the constant. As a result, the *Vc* value for geopolymer concrete requires a different approach from the conventional *Vc* equation, according to SNI. This is because the presence of the constant has been shown to make the calculated *Vc* value more in line with the *Vc* of the test results.

Aside from the constitutive model equation for shear-designed capacity, the crack pattern of the beam specimens was also observed. In this paper, the researcher uses the latest digital image correlation method. Basically, instead of marking the beam with uniform squares, it is marked with abstract dots so that the software will scan its deformation. Therefore, this deformation will ultimately show in a percentage. Several open resources are available to conduct this method, but this paper uses GOM by ZEUSS Quality Suite.

The observation of shear failure crack patterns in geopolymer beams is not much different from the results of previous studies. In several studies that also observed shear failure of geopolymer-reinforced beams, the crack pattern was not pure shear failure even though the beams were designed for the shear failure condition. However, in observing the crack patterns that appeared, flexural cracks also formed along the center of the beam [12,14]. This may indicate that geopolymer concrete has a different crack pattern from Portland cement concrete.

4. Conclusions

Comprehensively, from all test specimens, the geopolymer beams are ductile because they are able to bear *Pu* test loads 2-3 times greater than *Pu* according to conventional shear capacity design calculations according to SNI standards. A regression approach was performed on the *Vc* value of concrete shear capacity made in 2 equation models, namely model 1 with a constant and model 2 without a constant. Model 1 produces a strong coefficient of determination of 0.74, while model 2 is only 0.45. This proves that the presence of a constant in the formula for planning the shear capacity of geopolymer concrete beams improves the modeling interpretation by 29%. It can be concluded that the calculation of *Vc* values for geopolymer concrete requires another approach that is not the same as the conventional *Vc* equation according to SNI because it is evident that the presence of constants makes the calculated *Vc* values more in line with the *Vc* of the test results. In addition, the value of the shear reinforcement ratio in geopolymer-reinforced beams is not always proportional to the *Pu* value. From the experimental test results, beam 1B could bear a higher *Pu*, but beam 1A could bear a larger deflection. Meanwhile, beam 1C had the smallest deflection, and *Pu*. For the flexural reinforcement ratio, beam 2B is more ductile than 1B with higher *Pu* and smaller deflection.

Acknowledgment

This research has been funded by ITS Research Grant: Penelitian Dana Departemen with a registered number of 2321/PKS/ITS/2023.

REFERENCES

[1] E. Gartner, H. Hirao, Cement and Concrete Research A review of alternative approaches to the reduction of CO2 emissions associated with the manufacture of the binder phase in concrete. Cem. Concr. Res. (2015).
DOI: https://doi.org/10.1016/j.cemconres.2015.04.012

[2] B. Singh, G. Ishwarya, M. Gupta, S.K. Bhattacharyya, Geopolymer concrete: A review of some recent developments. Constr. Build. Mater. **85**, 78-90 (2015).
DOI: https://doi.org/10.1016/j.conbuildmat.2015.03.036

[3] K.H. Mo, U.J. Alengaram, M.Z. Jumaat, Structural performance of reinforced geopolymer concrete members: A review. Constr. Build. Mater. **120**, 251-264 (2016).
DOI: https://doi.org/10.1016/j.conbuildmat.2016.05.088

[4] A.A.K. Sharba, H.D. Hussain, Shear strength and Characterization of Reinforced Concrete Deep Beams – A Shear strength and Characterization of Reinforced Concrete Deep Beams – A Review. no. March (2021).
DOI: https://doi.org/10.1088/1757-899X/1076/1/012122

[5] C. Ma, A. Zawawi, W. Omar, Structural and material performance of geopolymer concrete: A review. Constr. Build. Mater. **186**, 90-102 (2018).
DOI: https://doi.org/10.1016/j.conbuildmat.2018.07.111

[6] M.S. Darmawan et al., Comparative Study Of Flexural Performance of Geopolymer and Portland Cement Concrete Beam. **23**, 95, 1-9 (2022).

[7] N.P. Rajamane, M.C. Nataraja, N. Lakshmanan, An introduction to geopolymer concrete. Indian Concr. J., no. November (2011).

[8] T. Phoo-ngernkham, C. Phiangphimai, N. Damrongwiriyanupap, S. Hanjitsuwan, J. Thumrongvut, P. Chindaprasirt, A Mix Design Procedure for Alkali-Activated High-Calcium Fly Ash Concrete Cured at Ambient Temperature. Adv. Mater. Sci. Eng. **2018** (2018).

[9] R. Bayuaji, A.K. Yasin, T.E. Susanto, M.S. Darmawan, A review in geopolymer binder with dry mixing method (geopolymer cement). in AIP Conference Proceedings **020022**, no. September (2017). DOI: https://doi.org/10.1063/1.5003505

[10] A. Kusbiantoro, M.S. Ibrahim, K. Muthusamy, A. Alias, The 3 rd International Conference on Sustainable Future for Human Security Development of sucrose and citric acid as the natural based admixture for fly ash based geopolymer. Procedia Environ. Sci. **17**, 596-602 (2013).
DOI: https://doi.org/10.1016/j.proenv.2013.02.075

[11] J.G. Jang, N.K. Lee, H.K. Lee, Fresh and hardened properties of alkali-activated fly ash/slag pastes with superplasticizers. Constr. Build. Mater. **50**, 169-176 (2014). [Online].
Available: https://www.sciencedirect.com/science/article/pii/S095006181300888X#b0090.

[12] N.S. Yacob, M.A. Elgawady, L.H. Sneed, A. Said, Shear strength of fly ash-based geopolymer reinforced concrete beams. Eng. Struct. **196**, May, 10929 (2019).
DOI: https://doi.org/10.1016/j.engstruct.2019.109298

[13] J.F. Hair, Jr., Multivariate Data Analysis, 5th ed. New Jersey, (2011).

[14] M.S. Darmawan, R. Bayuaji, H. Sugihardjo, H. Sugihardjo, N.A. Husin, R.B.A. Affandhi, Shear Strength of Geopolymer Concrete Beams Using High Calcium Content Fly Ash in a Marine Environment. Buildings **9**, 98, 1-13 (2019).
DOI: https://doi.org/10.3390/buildings9040098